ARTICLE

Coordination Chemistry and Structural Rearrangements of the $Me_2PCH_2AlMe_2$ Ambiphilic Ligand

Received 00th January 20xx,
Accepted 00th January 20xx

DOI: 10.1039/x0xx00000x

Katarina Paskaruk, David J. H. Emslie,* James F. Britten

Reaction of 2 equivalents of $(Me_2PCH_2AlMe_2)_2$ with $[\{RhCl(cod)\}_2]$ (cod = 1,5-cyclooctadiene) afforded $[\{\kappa^2\textit{P,P}\text{-}(Me_3AlCl)MeAl(CH_2PMe_2)_2\}Rh(cod)]$ (**1**), which features a κ^2-coordinated bis(phosphino)aluminate anion. In compound **1**, an Al–Cl substituent bridges to a molecule of $AlMe_3$, which could be removed in vacuo to provide $[\{\kappa^2\textit{P,P}\text{-}ClMeAl(CH_2PMe_2)_2\}Rh(cod)]$ (**2**). By contrast, reaction of 1 equiv. of $(Me_2PCH_2AlMe_2)_2$ with $[\{RhCl(cod)\}_2]$ yielded $[Rh(cod)(\mu\text{-}Cl)(Me_2PCH_2AlMe_2)]$ (**3**) as the major product, where the phosphine donor of an intact $Me_2PCH_2AlMe_2$ ligand is coordinated to rhodium and a chloride ligand bridges between Rh and Al. $[Rh(cod)(\mu\text{-}Cl)(Me_2PCH_2AlClMe)]$ (**3A**) and **2** were also formed as minor products. The aforementioned reactions were carried out in benzene or toluene, whereas the 1:1 reaction of $(Me_2PCH_2AlMe_2)_2$ with $[\{RhCl(cod)\}_2]$ in THF afforded $[\{Rh(\mu\text{-}CH_2PMe_2)(cod)\}_2]$ (**4**). Reactions of $(Me_2PCH_2AlMe_2)_2$ with iridium(I), gold(I) and platinum(II) precursors were also explored. A 1:1 reaction of $(Me_2PCH_2AlMe_2)_2$ with $[\{IrCl(cod)\}_2]$ afforded $[\{\kappa^2\textit{P,P}\text{-}Cl_2Al(CH_2PMe_2)_2\}Ir(cod)]$ (**5**) as one of two major phosphine-containing products; unlike **3**, this compound features two chlorine substituents on aluminium. For comparison, the rhodium analogue of **5**, $[\{\kappa^2\textit{P,P}\text{-}Cl_2Al(CH_2PMe_2)_2\}Rh(cod)]$ (**6**), was also synthesized via the 1:1 reaction of $\{ClAl(CH_2PMe_2)_2\}_2$ with $[\{RhCl(cod)\}_2]$. Reactions of $(Me_2PCH_2AlMe_2)_2$ with [LAuCl] (L = CO or SMe_2) or $[PtCl_2(cod)]$ also resulted in chloride-methyl group exchange between the transition metal and aluminium. However, these reactions generated free $(Me_2PCH_2AlClMe)_2$ accompanied by gold and ethane, or $[PtMe_2(cod)]$, respectively. Reaction of 1.5 equivalents of $(Me_2PCH_2AlMe_2)_2$ with $[PtMe_2(cod)]$ at 75 °C afforded zwitterionic $[(PtMe\{\mu\text{-}\kappa^1\textit{P}\text{:}\kappa^2\textit{P,P}\text{-}MeAl(CH_2PMe_2)_3\})_2]$ (**7**) which features two tris(phosphino)aluminate anions bridging between PtMe units. Compounds **1**-**2**, **3**/**3A**, **4**-**7** and $(Me_2PCH_2AlClMe)_2$ were crystallographically characterized.

Introduction

Transition metal complexes bearing ambiphilic ligands, that is ligands featuring one or more Lewis basic donor as well as a Lewis acidic acceptor, have been of great interest in recent years. These ligands are noteworthy due to the ability of the Lewis acid to interact with the metal centre, influencing the d-electron count, yielding compounds with unusual coordination geometries, and modulating the amount of electron density at the metal centre. Furthermore, the pendent Lewis acid can coordinate to substrates or co-ligands, or abstract co-ligands to form coordinatively-unsaturated species.[1-5] The majority of transition metal complexes featuring ambiphilic ligands contain borane Lewis acids. By comparison, alane-containing ambiphilic ligand complexes are far rarer,[6-42] despite the increased Lewis acidity of tris(hydrocarbyl)alanes relative to tris(hydrocarbyl)boranes.[43-45] Of these ligands, only three examples with a single phosphine donor have been utilized for the synthesis of transition metal complexes: $R_2P(NR'')AlR'_2$,[6-9,46] $Me_2PCH_2AlMe_2$,[10-12] and $Mes_2PC(=CHPh)Al^tBu_2$.[13-15]

Labinger and Miller *et al.* explored the reactivity of $R_2PN(R'')AlR'_2$ (primarily with R = Ph, R' = Me or Et, and R'' = ^{t}Bu) with iron[7,8] and manganese[6,9] complexes bearing carbonyl and either methyl or hydride ligands, demonstrating the ability of ambiphilic ligands to promote the formation of new C–C or C–H bonds. For example, reaction of $Ph_2PN(^tBu)AlEt_2$ with $[CpFe(CO)_2Me]$ afforded an iron complex containing a 5-membered CMe–O–$AlEt_2$–N^{t}Bu–PPh_2 ring coordinated to iron via C and O (A in Figure 1). This complex slowly isomerized to form an acyl complex featuring a 6-membered Fe–CMe=O–$AlEt_2$–N^{t}Bu–PPh_2 metallacycle (B in Figure 1). Similarly, reaction of $Ph_2PN(^tBu)AlR'_2$ (R' = Me or Et) with $[HMn(CO)_5]$ afforded a complex analogous to A in Figure 1, and for R = Me, this complex reacted with an additional equivalent of $Ph_2PN(^tBu)AlMe_2$ to afford C in Figure 1. These manganese complexes were proposed not to result from direct 1,1-insertion, given that a phosphonium salt was formed initially.

Zargarian *et al.* reported the use of the ambiphilic ligand precursor $(Me_2PCH_2AlMe_2)_2$ for the synthesis of nickel complexes.[10] A mixture of $(Me_2PCH_2AlMe_2)_2$ and [(1-Me-Ind)NiMe(PPh_3)] (Ind = indenyl) was used to facilitate the catalytic oligomerization of $PhSiH_3$. The active species was proposed to be $[(1\text{-Me-Ind})NiMe(Me_2PCH_2AlMe_2)]$, and the pendant alane was suggested to play an important role in

Department of Chemistry, McMaster University, 1280 Main Street West, Hamilton, Ontario, L8S 4M1, Canada. E-mail: emslied@mcmaster.ca

† Electronic Supplementary Information (ESI) available: NMR spectra and tables of crystallographic data. See DOI: 10.1039/x0xx00000x. CCDC 2184238-2184245 contain the supplementary crystallographic data for **1**-**7** and $(Me_2PCH_2AlClMe)_2$, respectively. These data can be obtained free of charge from The Cambridge Crystallographic Data Centre via www.ccdc.cam.ac.uk/data_request/cif.

catalysis. Although the aforementioned active species was not observed, the Lewis base adduct [(1-Me-Ind)NiMe{$Me_2PCH_2AlMe_2(NEt_3)$}] (D in Figure 1) was spectroscopically observed upon the addition of excess NEt_3. Additionally, rhodium $Me_2PCH_2AlMe_2$ complexes were reported by Fontaine et al.[11,12] These complexes include [Cp*RhMe$_2${$Me_2PCH_2AlMe_2$(L)}] {L = DMSO (E in Figure 1) or PMe_3} and [Cp*RhMe$_2$($Me_2PCH_2AlMe_2$)], and heating the DMSO adduct in the presence of 2 equiv. of $AlMe_3$ and 1 equiv. of $(Me_2PCH_2AlMe_2)_2$ afforded zwitterionic [Cp*RhMe{$(Me_2PCH_2)_2AlMe_2$)].[11]

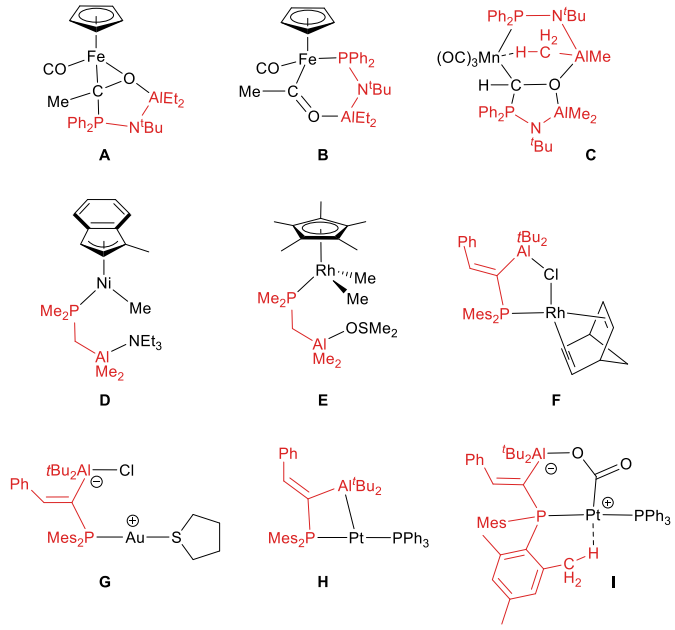

Figure 1. Complexes featuring monophosphine-alane ambiphilic ligands.

More recently, coordination of the $Mes_2PC(=CHPh)Al^tBu_2$ ligand to rhodium, palladium, gold and platinum was reported. Reactions with [{Rh(μ-Cl)(nbd)}$_2$] and [{Pd(μ-Cl)(allyl)}$_2$] afforded complexes in which a chloride ligand bridges between the transition metal and aluminium (e.g. F in Figure 1), whereas the reaction with [AuCl(THT)] (THT = tetrahydrothiophene) afforded a zwitterion in which the chloride anion has been abstracted by the alane (G in Figure 1).[13] Complexes in which the alane is coordinated to the transition metal were accessed via reactions with [Au(C_2Ph)]$_n$, [Au(THT)(C_6F_5)],[14] [Pd(η^3-C_3H_5)(μ-Cl)}$_2$],[13,14] or [Pt(C_2H_4)(PPh_3)$_2$], and the platinum complex [{$Mes_2PC(=CHPh)Al^tBu_2$}Pt(PPh_3)] (H in Figure 1) was shown to engage in cooperative reactivity resulting in CO_2 (I in Figure 1) and CS_2 fixation, and H_2 and $PhC(O)NH_2$ activation.[15]

As research into small alane-containing ambiphilic ligands is in its infancy, we sought to further research the coordination of $Me_2PCH_2AlMe_2$ to late transition metal complexes, with a focus on probing the ability of this flexible and sterically unencumbered ligand to interact with co-ligands (e.g. Cl^- or Me^-), and the circumstances under which the ligand engages in reactivity at the aluminium–alkyl linkages.

Results and discussion

Reaction of 2 equivalents of $(Me_2PCH_2AlMe_2)_2$[47] with [{Rh(μ-Cl)(cod)}$_2$] (cod = 1,5-cyclooctadiene) in benzene or toluene at room temperature afforded [{κ^2*P,P*-(Me_3AlCl)$MeAl(CH_2PMe_2)_2$}Rh(cod)] (**1**; Scheme 1), with a $^{31}P\{^1H\}$ NMR chemical shift of –5.83 ppm ($^1J_{103Rh-31P}$ = 138 Hz). This complex does not contain two $Me_2PCH_2AlMe_2$ ligands. Rather, it contains a bidentate bis(phosphino)aluminate ligand which is κ^2-coordinated to rhodium via two phosphine arms; this bidentate ligand can be considered to be comprised of a $ClMeAl(CH_2PMe_2)_2$ anion in which the chloride substituent bridges to a molecule of $AlMe_3$.

An X-ray crystal structure of **1** (Figure 2) shows the expected square planar geometry at rhodium (angles in the square plane range from 84.85° to 92.81°), with Rh–P distances of 2.3283(7) and 2.3195(6) Å, and Rh–C distances ranging from 2.212(2) to 2.246(2) Å. The Al(1)–Cl(1)–Al(2) angle is 113.85(3)°, and both aluminium centres adopt a slightly distorted tetrahedral geometry. The Al(1)–Cl and Al(2)–Cl distances are 2.3038(9) and 2.416(1) Å, respectively, indicating that chloride is more tightly bound by the aluminium centre of the ligand backbone {Al(1)}, although both distances are elongated compared the sum of the covalent radii (2.23 Å).[48] Additionally, Al(1) is more pyramidalized, with the sum of the C–Al–C bond angles equal to 340.3(2)°, compared to 348.2(3)° for Al(2).

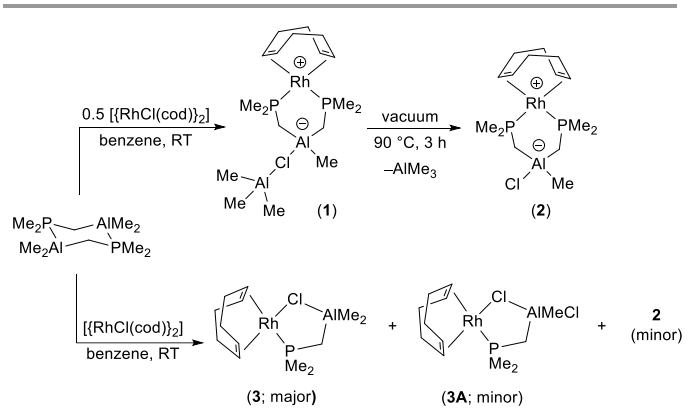

Scheme 1. Reactivity of $(Me_2PCH_2AlMe_2)_2$ with [{RhCl(cod)}$_2$].

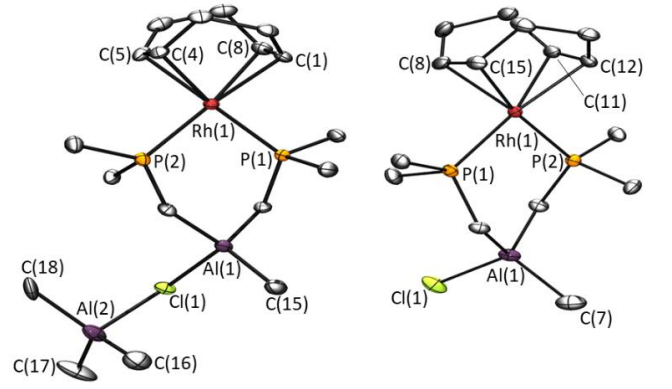

Figure 2. X-ray crystal structures of **1** (left) and **2** (right). Ellipsoids are set at 50% and hydrogen atoms are omitted for clarity. In **2**, the Cl and CH_3 groups on Al(1) are disordered (80:20) over two positions, and only the major one of these is shown.

Solid **1** loses $AlMe_3$ slowly under vacuum at room temperature, or more rapidly at elevated temperature, affording [{κ²*P,P*-ClMeAl(CH_2PMe_2)$_2$}Rh(cod)] (**2**; Scheme 1). The structure of **2** was confirmed by NMR spectroscopy and X-ray crystallography (Figure 2), and is analogous to that of **1**, although the Al–Cl distance in **2** is considerably shorter, at 2.199(1) Å. The Rh–P distances are 2.3249(5) and 2.3348(5) Å for P(1) and P(2), respectively, and the Rh–C distances range from 2.209(2) to 2.250(2) Å. Compared with the structure of **1**, aluminium is more pyramidalized, with the sum of the C–Al–C bond angles equal to 332.5(4)°.

Room temperature ^{1}H and ^{13}C NMR spectra of **1** in CD_2Cl_2 are indicative of apparent C_{2v} symmetry, despite approximate C_s symmetry in the solid state. For example, the P*Me*$_2$ and P*CH*$_2$Al groups each gave rise to just one ^{1}H or ^{13}C NMR signal. Furthermore, only a single peak was observed for the methyl substituents on the two inequivalent aluminium centres. By contrast, low temperature ^{1}H and ^{13}C NMR spectra revealed separate AlMe and $AlMe_3$ signals, as well as separation of the PMe and PCH_2Al ^{1}H NMR signals into two singlets and two doublets, respectively. The apparent C_{2v} symmetry at room temperature is presumably due to a fluxional process involving initial $AlMe_3$ or $ClAlMe_3^-$ dissociation. For example, (a) reversible $AlMe_3$ dissociation followed by methyl group abstraction to afford undetected [{κ²*P,P*-ClAl(CH_2PMe_2)$_2$}Rh(cod)][$AlMe_4$], or (b) reversible $AlMe_3Cl^-$ dissociation followed by transfer of a methyl group back to the alane in the ligand backbone, affording undetected [{κ²*P,P*-Me_2Al(CH_2PMe_2)$_2$}Rh(cod)] and Me_2AlCl. In keeping with either of these mechanisms, room temperature ^{1}H NMR spectra of **2** show the expected C_s symmetry, but addition of a sub-stoichiometric amount (<0.1 equiv.) of $AlMe_3$ resulted in a switch to apparent C_{2v} symmetry.

The bidentate bis(phosphino)aluminate ligands in **1** and **2** are relatives of the $Me_2Al(CH_2PMe_2)_2^-$ ligand in Fontaine's [Cp*{κ²*P,P*-Me_2Al(CH_2PMe_2)$_2$}RhMe]. These aluminate ligands are heavy analogues of Peters' bis(phosphino)borate ligands, $R'_2B(CH_2PR_2)_2^-$,[49] and to our knowledge, **1** and **2** are only the second and third structurally characterized examples of transition metal $R'_2Al(CH_2PR_2)_2^-$ complexes.

In contrast to the 2:1 reaction of ($Me_2PCH_2AlMe_2$)$_2$ with [{Rh(μ-Cl)(cod)}$_2$], the 1:1 reaction (in benzene or toluene) afforded an orange-brown solution with some suspended solid. Three products were observed in the ^{31}P{^{1}H} NMR spectrum of the reaction mixture, with chemical shifts at 7.12 ppm (major; >80%), and 4.56 and –5.89 ppm (minor), in all cases with similar $^1J_{Rh,P}$ coupling constants of 133.6-138.4 Hz. Based on the ^{1}H, ^{31}C and ^{31}P NMR data, the latter minor product (^{31}P = –5.89 ppm) is assigned to compound **2**.

Slow evaporation of the reaction solution afforded a dark precipitate as well as golden-yellow crystals which contained a 68:32 mixture of [Rh(cod)(μ-Cl)($Me_2PCH_2AlMe_2$)] (**3**) and [Rh(cod)(μ-Cl)($Me_2PCH_2AlClMe$)] (**3A**); the unit cell contains two independent molecules, one of which is not disordered and contains only compound **3** (Figure 3), and one of which is disordered between **3** and **3A** in an 36:64 ratio. Compound **3** contains an intact $Me_2PCH_2AlMe_2$ ligand, with a chloride co-ligand bridging between Rh and Al. The non-disordered molecule of **3** features Rh–P and Rh–Cl distances of 2.2967(3) and 2.4176(3) Å, respectively, and Rh–C distances ranging from 2.104(1) to 2.253(1) Å. The Al–Cl bond distance is 2.3427(4) Å, which is similar to that in [Rh(nbd)(μ-Cl)(Mes_2PC(=CHPh)Al^{t}Bu$_2$)] (nbd = 2,5-norbornadiene),[13] and the sum of the C–Al–C bond angles is 346.70(9)°. Dissolution of these crystals afforded two ^{31}P NMR signals at 7.12 and 4.56 ppm in an approximate 2:1 ratio, indicating that **3** is the major product in the 1:1 reaction of ($Me_2PCH_2AlMe_2$)$_2$ with [{Rh(μ-Cl)(cod)}$_2$], and **3A** is the minor product with a ^{31}P NMR chemical shift of 4.56 ppm (Scheme 1).

The reaction between ($Me_2PCH_2AlMe_2$)$_2$ and [{Rh(μ-Cl)(cod)}$_2$] is solvent-dependent, and afforded [{Rh(μ-CH_2PMe_2)(cod)}$_2$] (**4**) {accompanied by $AlMe_2Cl$(THF)} when the reaction was carried out with 1:1 stoichiometry in THF (Scheme 2). This process likely involves initial formation of compound **3**, and consistent with this hypothesis, **3** (as the major product in the mixture formed from the 1:1 reaction of ($Me_2PCH_2AlMe_2$)$_2$ with [{Rh(μ-Cl)(cod)}$_2$] in benzene; *vide supra*) rapidly converted to **4** upon dissolution in THF.

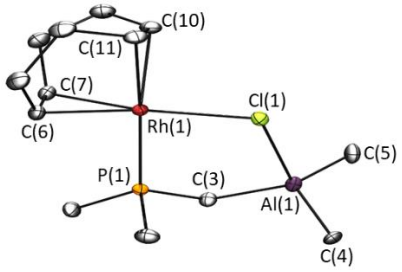

Figure 3. X-ray structure of **3** from crystals containing [Rh(cod)(μ-Cl)($Me_2PCH_2AlMe_2$)] (**3**) and [Rh(cod)(μ-Cl)($Me_2PCH_2AlClMe$)] (**3A**) in a 68:32 ratio. The unit cell contains two independent molecules; one is a non-disordered molecule of **3**, whereas the other is disordered between **3** and **3A** in a 36:64 ratio. This figure shows only the non-disordered molecule of **3**. Ellipsoids are set at 50% and hydrogen atoms have been omitted for clarity.

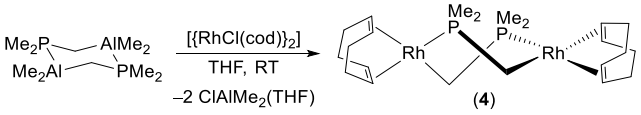

Scheme 2. Formation of **4** in THF.

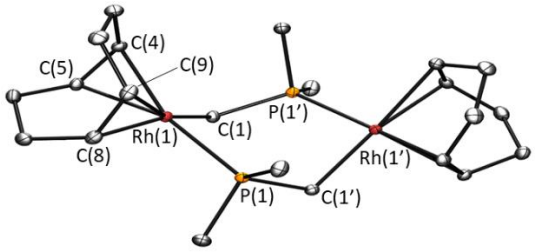

Figure 4. X-ray crystal structure of **4**. Ellipsoids are set to 50% probability. Hydrogen atoms have been omitted for clarity.

Red X-ray quality crystals of **4** were obtained by layering the reaction mixture with pentane and cooling to –30 °C, and revealed two bridging $CH_2PMe_2^-$ anions, with each rhodium centre coordinating to the carbon atom of one $CH_2PMe_2^-$ ligand

and the phosphorus atom of the other (Figure 4). This structure is similar to that observed for the rhodium(III) complex [{Cp*RhMe(μ-CH_2PMe_2)}$_2$].[11] For example, both adopt a twist-boat conformation of the 6-membered $Rh_2C_2P_2$ ring, and the Rh–C distances are similar (2.108(1) Å in **4**, compared with 2.101(7) and 2.095(7) Å in the rhodium(III) complex).

To explore the generality of the reactivity observed between $(Me_2PCH_2AlMe_2)_2$ and [{RhCl(cod)}$_2$] in arene solvents, analogous reactions were carried out using [{IrCl(cod)}$_2$]. In the 1:1 reaction, two phosphorus-containing products were formed in an approximate 1:1 ratio, with ^{31}P NMR signals at –13.08 and –48.10 ppm. Attempts to isolate and identify the product giving rise to the lower frequency ^{31}P NMR signal were unsuccessful. However, the compound with a ^{31}P NMR signal at –13.08 ppm was isolated from a 2:1 mixture of [{IrCl(cod)}$_2$] and $(Me_2PCH_2AlMe_2)_2$, recrystallized from 1,2-difluorobenzene/hexanes, and was identified by X-ray diffraction as [{κ^2*P,P*-$Cl_2Al(CH_2PMe_2)_2$}Ir(cod)] (**5**; Scheme 3). The new bis(phosphino)aluminate ligand in **5** is related to that in compound **2**, except that aluminium has two chlorine substituents. The rhodium analogue of **5**, [{κ^2*P,P*-$Cl_2Al(CH_2PMe_2)_2$}Rh(cod)] (**6**), was also synthesized via the 1:1 reaction of $\{ClAl(CH_2PMe_2)_2\}_2$[47] with [{RhCl(cod)}$_2$] (Scheme 3). The solid state structures of **5** and **6** (Figure 5) are analogous to that of **2**. The M–C distances are 2.225(2) and 2.196(2) Å in **5**, and 2.2546(7) and 2.2190(7) Å in **6**, and the M–P and M–Cl distances are 2.3208(4) and 2.1789(6) in **5**, and 2.3175(2) and 2.1829(3) in **6**.

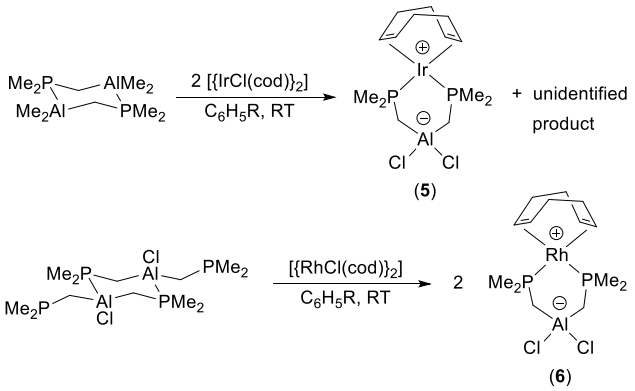

Scheme 3. Formation of complexes **5** and **6**, bearing the $Cl_2Al(CH_2PMe_2)_2^-$ ligand.

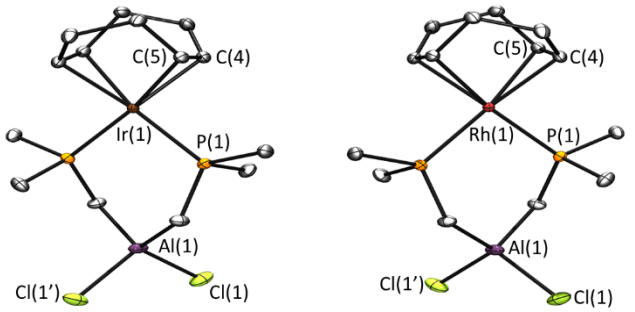

Figure 5. X-ray crystal structures of **5** (left) and **6** (right). Ellipsoids are set at 50% probability. Hydrogen atoms have been omitted for clarity.

To extend the reactivity of $(Me_2PCH_2AlMe_2)_2$ beyond group 9 metals, a solution of $(Me_2PCH_2AlMe_2)_2$ (0.5 equiv.) was added to [ClAu(CO)] (Scheme 4), affording an ink-blue mixture within seconds, indicative of gold colloid formation. This was followed by precipitation of a black powder and deposition of a thin gold mirror on the walls of the reaction flask. Powder X-ray diffraction of the precipitated solid confirmed its identity as elemental gold. The remaining clear, colourless reaction solution was analysed by ^{1}H and ^{31}P NMR spectroscopy and shown to contain ethane as well as $(Me_2PCH_2AlClMe)_2$ as an approx. 2:1 mixture of diastereomers; crystals of the *meso* diastereomer of $(Me_2PCH_2AlClMe)_2$ were obtained by slow evaporation of the supernatant, and the structure was confirmed by X-ray diffraction (Figure 6). These products are indicative of exchange of chloride and methyl groups between gold and aluminium, to generate an unstable gold methyl species which undergoes ethane reductive elimination[50-52] to deposit elemental gold. This reactivity contrasts that of $Mes_2PC(=CHPh)Al^tBu_2$,[13] {(*o*-$Ph_2P)C_6H_4$}$_2$AlCl[16] and {(*o*-$Ph_2P)C_6H_4$}$_3$Al[17] with gold(I) chloride complexes, which resulted in chloride abstraction to afford stable zwitterionic gold(I) products.

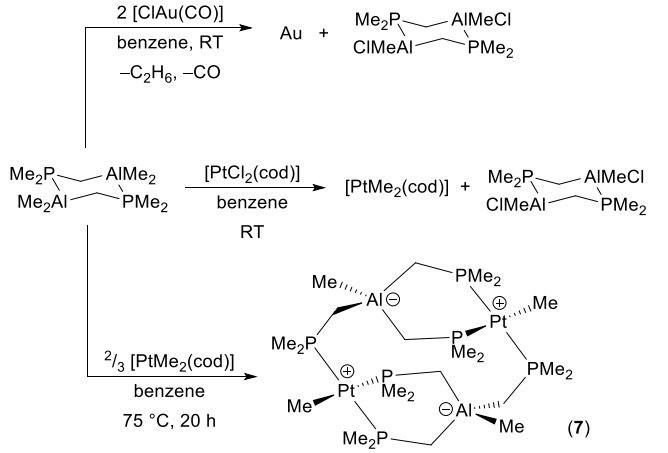

Scheme 4. Reactivity of $(Me_2PCH_2AlMe_2)_2$ with gold and platinum precursors.

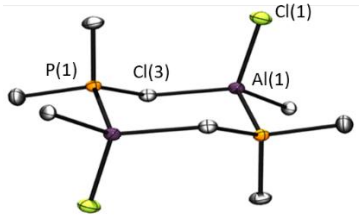

Figure 6. X-ray crystal structure of the *meso* diastereomer of $(Me_2PCH_2AlClMe)_2$. Ellipsoids are set at 50% probability. Hydrogen atoms have been omitted for clarity.

The reactivity of $(Me_2PCH_2AlMe_2)_2$ with platinum precursors containing either chloride or methyl ligands was also explored, in light of the varied reactivity observed with late transition metal chloride complexes, and to probe the behaviour of the $Me_2PCH_2AlMe_2$ ligand in the presence of methyl co-ligands.

When 1 equiv. of $(Me_2PCH_2AlMe_2)_2$ was added to a solution of $[PtCl_2(cod)]$, chlorine-methyl exchange between platinum and aluminium was again observed, affording $(Me_2PCH_2AlClMe)_2$ and $[PtMe_2(cod)]$ (Scheme 4). By contrast, no reaction was observed between $(Me_2PCH_2AlMe_2)_2$ (0.5 or 1.5 equiv.) and $[PtMe_2(cod)]$ at room temperature. However, when the mixture was heated to 75 °C, a new phosphine-containing product was generated over the course of 20 hours (in higher yield in the 1.5:1 reaction), accompanied by the formation of approx. 4 equiv. of free $AlMe_3$ (Scheme 4).

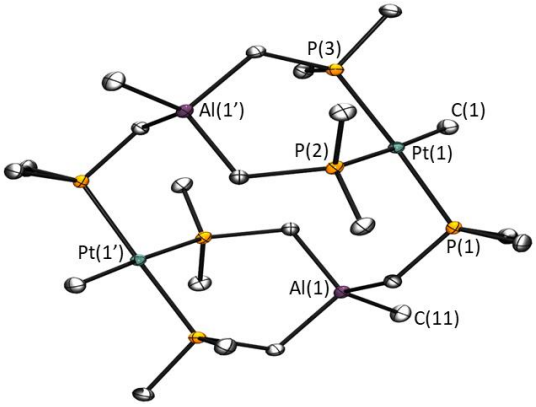

Figure 6. X-ray crystal structure of **7**. Ellipsoids are set at 50%. Hydrogen atoms have been omitted for clarity.

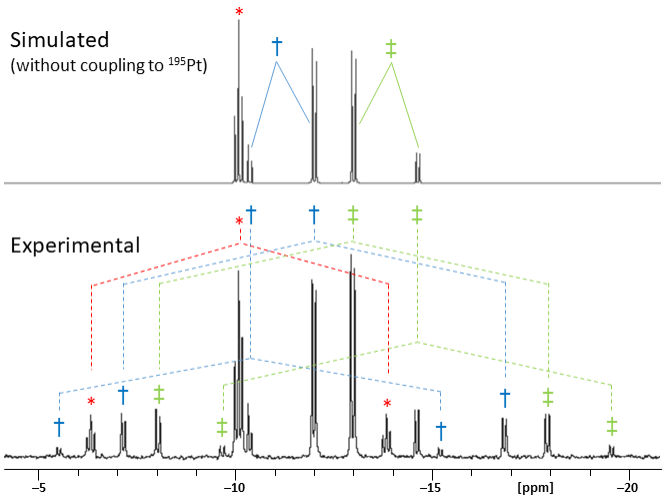

Figure 7. Experimental and simulated $^{31}P\{^1H\}$ NMR spectra of **7**. In the simulated spectrum, coupling to ^{195}Pt was not included. The *, † and ‡ symbols correspond to the three inequivalent phosphine donors attached to each platinum centre; * is *trans* to a methyl ligand, whereas † and ‡ are *trans* to one another. In the experimental spectrum, dashed lines highlight the position of ^{195}Pt-satellites relative to the central peak.

The new product was isolated as clear colourless crystals by slow evaporation of a benzene solution, and was identified by X-ray crystallography (Figure 6) as zwitterionic $[(PtMe\{\mu\text{-}\kappa^1P{:}\kappa^2P,P\text{-}MeAl(CH_2PMe_2)_3\})_2]$ (**7**). Compound **7** features two tridentate tris(phosphino)aluminate anions bridging between square planar platinum centres, with each ligand κ^2-coordinated to one platinum, and κ^1-coordinated to the other. Each platinum centre also retains one methyl ligand. The Pt–C distance is 2.115(1) Å, and the Pt–P distances are 2.3144(3) and 2.3211 (3) Å for the phosphines *trans* to one another, and 2.3297(3) Å for the phosphine *trans* to the methyl group. The geometry around the platinum centre is square planar, with P–Pt–P angles of 95.24(1)° and 92.98(1)°, and smaller C–Pt–P angles of 87.05(4)° and 84.91(4)°.

The $^{31}P\{^1H\}$ NMR spectrum of **7** features three signals due to the three inequivalent phosphine donors (each with ^{195}Pt satelites; $^1J_{P,Pt}$ is ~2400 Hz for the phosphines *trans* to one another, and 1830 Hz for the phosphine *trans* to the methyl group), and is complicated by second order effects. Thus, the ^{31}P-^{31}P coupling constants (and ^{31}P NMR shifts) were found via simulation; the *cis* $^2J_{P\text{-}P}$ couplings are 22 and 23 Hz, whereas the *trans* $^2J_{P\text{-}P}$ coupling is 398 Hz (Figure 7). To the best of our knowledge, compound **7** is the first example of a transition metal tris(phosphino)aluminate $\{R'Al(CH_2PR_2)_3^-\}$ complex, and it is interesting that the formation of this ligand was favoured, even when an excess of $[PtMe_2(cod)]$ was present (e.g. in the reaction between 0.5 equiv. of $(Me_2PCH_2AlMe_2)_2$ and $[PtMe_2(cod)]$).

Summary and Conclusions

Reactions between $(Me_2PCH_2AlMe_2)_2$ and late transition metal complexes led to five distinct outcomes:

(1) Complexation of an intact $Me_2PCH_2AlMe_2$ ambiphilic ligand; one equiv. of $(Me_2PCH_2AlMe_2)_2$ reacted with $[\{RhCl(cod)\}_2]$ in arene solvents to afford $[Rh(cod)(\mu\text{-}Cl)(Me_2PCH_2AlMe_2)]$ (**3**) as the major product.

(2) In-situ generation of a bis(phosphino)aluminate ligand. This outcome was observed in the 2:1 reaction between $(Me_2PCH_2AlMe_2)_2$ and $[\{RhCl(cod)\}_2]$, and the 1:1 and 1:2 reactions between $(Me_2PCH_2AlMe_2)_2$ and $[\{IrCl(cod)\}_2]$, generating $[\{\kappa^2P,P\text{-}XMeAl(CH_2PMe_2)_2\}Rh(cod)]$ {X = $ClAlMe_3$ (**1**) or Cl (**2**)} or $[\{\kappa^2P,P\text{-}Cl_2Al(CH_2PMe_2)_2\}Ir(cod)]$ (**5**), respectively.

(3) Formation of a dimethylphosphinomethyl complex; reactions between $(Me_2PCH_2AlMe_2)_2$ and $[\{RhCl(cod)\}_2]$ in THF afforded $[\{Rh(\mu\text{-}CH_2PMe_2)(cod)\}_2]$ (**4**). Compound **3** also rapidly converted to **4** in THF.

(4) Chloride-methyl exchange to afford free $(Me_2PCH_2AlClMe)_2$; reactions of $(Me_2PCH_2AlMe_2)_2$ with [(CO)AuCl] or $[PtCl_2(COD)]$ provided free $(Me_2PCH_2AlClMe)_2$ accompanied by gold and ethane, or $[PtMe_2(COD)]$, respectively.

(5) In-situ generation of a tris(phosphino)aluminate ligand; reaction of $(Me_2PCH_2AlMe_2)_2$ with $[PtMe_2(cod)]$ yielded $[(PtMe\{\mu\text{-}\kappa^1P{:}\kappa^2P,P\text{-}MeAl(CH_2PMe_2)_3\})_2]$ (**7**).

These reactions highlight the ability of $Me_2PCH_2AlMe_2$ to serve as an ambiphilic ligand, but also the propensity of this ligand to engage in reactivity involving the $Al\text{–}C_{alkyl}$ bonds,[11,53] and the sensitivity of this reactivity to the identity of the transition metal, as well as the co-ligands (Cl vs Me), reaction stoichiometry, and solvent (arene solvents vs THF). However, it is important to note that ambiphilic ligands featuring $Al\text{–}C_{alkyl}$ linkages do not always engage in reactivity at the Al–C bonds. For example, the Al–C linkages in $Ph_2P(N^tBu)AlR_2$ (R = Me or Et)[6-

[9] and $Mes_2PC(CHPh)Al^tBu_2$[13-15] remained in intact in various transition metal complexes (*vide supra*). Additionally, a tridentate PPAl ligand (FcPPAl) containing an $ArAlMe_2$ moiety was used to form [{Pt(FcPPAl)}$_2$], [Pt(L)(FcPPAl)] [L= norbornene, C_2H_4, C_2Ph_2, CO] and [PtH_2(FcPPAl)], and in all cases, the FcPPAl ligand remained intact.[21]

Compounds **1**, **2** and **5** are rare examples of bis(phosphino)aluminate {$R'_2Al(CH_2PR_2)_2^-$} complexes, and to the best of our knowledge, compound **7** is the first example of a transition metal tris(phosphino)aluminate {$R'Al(CH_2PR_2)_3^-$} complex. It is remarkable that this ligand was assembled selectively via the reaction of $(Me_2PCH_2AlMe_2)_2$ with [$PtMe_2$(cod)], especially considering that the lithium salt of the $MeAl(CH_2PMe_2)_3^-$ anion has been reported to undergo rapid ligand redistribution to form $Me_2Al(CH_2PMe_2)_2^-$ and $Al(CH_2PMe_2)_4^-$.[54]

Conflicts of interest

There are no conflicts to declare.

Acknowledgements

D. J. H. E. thanks NSERC of Canada for a Discovery Grant.

Experimental

General Details: Experiments were carried out in an argon-filled MBraun UniLab glove box or on a double manifold high vacuum line using standard techniques. The metal complexes [{RhCl(cod)}$_2$] and [{IrCl(cod)}$_2$] were purchased from Strem Chemicals. [$PtMe_2$(cod)][55] was prepared via literature procedure. [AuCl(CO)] and [$PtCl_2$(cod)] were purchased from Strem Chemicals. The ligand precursors $(Me_2PCH_2AlMe_2)_2$ and $\{(Me_2PCH_2)_2AlCl\}_2$ were prepared via reactions of Me_2AlCl or $AlCl_3$ with $LiCH_2PMe_2$.[47] Benzene, hexanes, pentane, tetrahydrofuran (THF), diethyl ether (Et_2O) were purchased from Sigma Aldrich, dried over sodium/benzophenone, and distilled under nitrogen. Toluene was purchased from Sigma Aldrich, dried over sodium metal and distilled. Anhydrous dichloromethane (DCM) was purchased from Sigma Aldrich, dried over molecular sieves (4 Å), and distilled. Deuterated solvents were purchased from Cambridge Isotope Laboratories; C_6D_6 (99.5%) was dried over sodium/benzophenone, distilled prior to use, and stored under argon. CD_2Cl_2 (99.8%) was dried over molecular sieves (4 Å), distilled prior to use, and stored under argon.

NMR spectroscopy (^{1}H, ^{13}C{^{1}H}, ^{31}P{^{1}H}, COSY, HSQC, HMBC, NOESY) was performed on Bruker AV-500 and AV-600 spectrometers. Spectra were obtained at 298 K unless otherwise indicated. All ^{1}H NMR spectra were referenced relative to $SiMe_4$ through a resonance of the protio impurity of the solvent used: C_6D_6 (δ 7.16 ppm), CD_2Cl_2 (δ 5.32 ppm) and d^8-toluene (δ 2.08 ppm, 6.97 ppm, 7.01 ppm, and 7.09 ppm). All ^{13}C NMR spectra were referenced relative to $SiMe_4$ through a resonance of the ^{13}C in the solvents: C_6D_6 (δ 128.06 ppm), CD_2Cl_2 (δ 54.00 ppm) and d^8-toluene (δ 20.43, 125.13, 127.96, 128.87, and 137.48 ppm). The ^{31}P NMR spectra were referenced using an external standard of 85% H_3PO_4 in D_2O (0.0 ppm). Relative concentrations of species were determined by integration of ^{1}H NMR spectra, unless otherwise indicated. The ^{31}P{^{1}H} NMR spectrum of **7** was simulated using the DAISY program in TopSpin 4.0.

Single-crystal X-ray crystallographic analyses were performed at 100 K (unless otherwise stated) on crystals coated in Paratone oil and mounted on a SMART APEX II diffractometer with a 3 kW sealed-tube Mo generator and SMART6000 CCD detector in the McMaster Analytical X-Ray (MAX) Diffraction Facility. Raw data was processed using XPREP (as part of the APEX v2.2.0 software), and solved by either direct (SHELXS-97)[56] or intrinsic (SHELXT)[57] methods. Structures were completed by difference Fourier synthesis and refined with full-matrix least-squares procedures based on F^2. In all cases, non-hydrogen atoms were refined anisotropically and hydrogen atoms were generated in ideal positions and then updated with each cycle of refinement, which was performed with SHELXL[58] in Olex2.[59]

Combustion elemental analyses were performed by Midwest Micro-labs in Indianapolis, the Analest facility at the University of Toronto, or the University of Calgary.

[{κ^2*P,P*-(Me_3AlCl)$MeAl(CH_2PMe_2)_2$}Rh(cod)] (1): A solution of $(Me_2PCH_2AlMe_2)_2$ (53.4 mg, 0.203 mmol) in 1 mL of benzene was added to [{RhCl(cod)}$_2$] (49.9 mg, 0.101 mmol) in 2 mL of benzene. The deep red solution was stirred at 25°C for 3 hours. NMR spectroscopy indicated a quantitative conversion to the product. The deep burgundy solution was evaporated to dryness in vacuo, and the resulting deep red solid was dried in vacuo for approx. 15 minutes. The product was then recrystallized from a concentrated solution of DCM at –30°C to obtain clear, red X-ray quality crystals of **1**, which were dried for 10 minutes *in vacuo*. The recrystallized yield was 53.1 mg (51 %). Compound **1** slowly loses $AlMe_3$ *in vacuo* at room temperature (~10% after 10 minutes; ~50% after 1h), so the $AlMe_3$ signal for the dried solid integrated to ~90% of the expected value, and a satisfactory elemental analysis was not obtained. **^{1}H NMR (600 MHz, 298K, CD_2Cl_2) δ:** 4.74 (s, 4H, C*H* (cod)), 2.29 (m, 8H, CH_2 (cod)), 1.30 (m, 12H, PMe_2), 0.36 (d, 4H, $^2J_{P\text{-}H}$ 10.2 Hz, PCH_2Al), –0.74 (bs, 12H, Al*Me* & ClAlMe_3)). **^{13}C{^{1}H} NMR (150.9 MHz, 298K, CD_2Cl_2) δ:** 93.7 (m, *C*H (cod)), 31.0 (s, *C*H_2 (cod)), 18.0 (t, $^1J_{P\text{-}C}$ 13 Hz, PMe_2), 11.9 (bs, P*C*H_2Al), –5.9 (bs, Al*Me* & AlMe_3). **^{31}P{^{1}H} NMR (242.9 MHz, 298K, CD_2Cl_2) δ:** –6.40 (d, $^1J_{Rh\text{-}P}$ 140.9 Hz).

[{κ^2*P,P*-$ClMeAl(CH_2PMe_2)_2$}Rh(cod)] (2): Compound **2** was obtained in a quantitative yield after heating solid [{κ^2*P,P*-(Me_3AlCl)$MeAl(CH_2PMe_2)_2$}Rh(COD)] (**1**) under vacuum at 90 °C for 3 hours. $C_{15}H_{31}AlClP_2Rh$ (438.70 g mol^{-1}): calcd. C 41.07 %, H 7.12 %; found C 41.21 %, H 7.30 %. **^{1}H NMR (600 MHz, 298K, C_6D_6) δ:** 4.32 (bs, 2H, C*H* (cod)), 4.22 (bs, 2H, C*H* (cod)), 1.7-1.9 (m, 8H, CH_2 (cod)), 1.03 (m, 6H, PMe_2), 0.89 (m, 6H, PMe_2), 0.55 (t, 2H, $^2J_{P\text{-}H}$ 12 Hz, PCH_2Al), 0.31 (t, 2H, $^2J_{P\text{-}H}$ 12 Hz, PCH_2Al), –0.02 (s, 3H, Al*Me*). **^{13}C{^{1}H} NMR (125.8 MHz, 298K, C_6D_6) δ:** 91.76 (d, $^1J_{Rh\text{-}C}$ 75 Hz, *C*H (cod)), 30.74 (s, *C*H_2 (cod)), 17.98 (m, PMe_2), 17.37 (m, PMe_2), 12.46 (bs, P*C*H_2Al), –4.58 (bs,

Al*Me*). **^{31}P{^{1}H} NMR (242.93 MHz, 298K, C_6D_6) δ:** –5.80 (d, $^{1}J_{Rh-P}$ = 139 Hz, *P*Me$_2$).

[Rh(cod)(μ-Cl)($Me_2PCH_2AlMe_2$)] (3) and [Rh(cod)(μ-Cl)($Me_2PCH_2AlClMe$)] (3A): A solution of $(Me_2PCH_2AlMe_2)_2$ (10.0 mg, 0.0379 mmol) in 0.3 mL of C_6D_6 was added to [{RhCl(cod)}$_2$] (18.7 mg, 0.0379 mmol) in 0.3 mL of C_6D_6. The reaction mixture became orange-brown and cloudy within seconds. NMR spectroscopy indicated that the major species in solution was **3** (82.5%), accompanied by 6.0% of **3A**, and 11.5% of **2**. The solution was decanted, and slow evaporation afforded golden-yellow crystals which were manually separated from a dark brown precipitate. X-ray diffraction indicated that the crystals contain a mixture of **3** (68%) and **3A** (32%). **NMR data for 3**: **^{1}H NMR (500 MHz, 298K, C_6D_6) δ:** 5.11 (m, 2H, C*H* (cod)), 3.20 (m, 2H, C*H* (cod)), 1.90 (m, 4H, C*H$_2$* (cod)), 1.51 (m, 4H, C*H$_2$* (cod)), 0.78 (d, 6H, $^{2}J_{P-H}$ = 9.4 Hz, P*Me$_2$*), 0.31 (d, 2H, $^{2}J_{P-H}$ 15 Hz, PC*H$_2$*Al), –0.05 (bs, 6H Al*Me$_2$*). **^{13}C{^{1}H} NMR (125.7 MHz, 298K, C_6D_6) δ:** 103.82 (m, *C*H (cod)), 68.81 (d, $^{2}J_{P-C}$ 15 Hz, *C*H (cod)), 33.23 (d, $^{3}J_{P-C}$ 3 Hz, *C*H$_2$ (cod)), 28.16 (d, $^{3}J_{P-C}$ 2 Hz, *C*H$_2$ (cod)), 15.50 (d, P*Me*, $^{1}J_{P-C}$ 26 Hz), 15.0 (bs, P*C*H$_2$Al), –5.45 (bs, Al*Me*). **^{31}P{^{1}H} NMR (202.5 MHz, 298K, C_6D_6) δ:** 7.14 (d, $^{1}J_{Rh-P}$ 136.0 Hz, *P*Me$_2$). **NMR data for 3A**: **^{1}H NMR (500 MHz, 298K, C_6D_6) δ:** 5.00 (m, 2H, C*H* (cod)), 3.14 (m, 2H, C*H* (cod)), 1.90 (m, 4H, C*H$_2$* (cod)), 1.51 (m, 4H, C*H$_2$* (cod)), 0.75 (d, 6H, $^{2}J_{P-H}$ = 9.4 Hz, P*Me$_2$*), 0.33 (d, 2H, $^{2}J_{P-H}$ 15 Hz, PC*H$_2$*Al), 0.05 (bs, 3H Al*Me*). **^{13}C{^{1}H} NMR (125.7 MHz, 298K, C_6D_6) δ:** 104.35 (m, *C*H (cod)), 69.37 (d, $^{2}J_{P-C}$ 15 Hz, *C*H (cod)), 33.08 (m, *C*H$_2$ (cod)), 28.02 (bs, *C*H$_2$ (cod)), 15.05 (d, $^{1}J_{P-C}$ 26 Hz, P*Me*), 13.5 (located from 2D NMR spectra, P*C*H$_2$Al), –5.45 (bs, Al*Me*). **^{31}P{^{1}H} NMR (202.5 MHz, 298K, C_6D_6) δ:** 4.59 (d, $^{1}J_{Rh-P}$ 133.6 Hz, *P*Me$_2$).

[{Rh(μ-CH_2PMe_2)(cod)}$_2$] (4): A solution of $(Me_2PCH_2AlMe_2)_2$ (20.3 mg, 0.0767 mmol) in 1 mL of THF was added to [{RhCl(cod)}$_2$] (37.8 mg, 0.0767 mmol) in 2 mL of THF. The bright red solution was stirred at 25°C for 1 hour. The solution was layered with 1 mL of pentane, and cooled to –30°C for 12 hours to obtain bright red x-ray quality crystals of **4**. The recrystallized yield was 22.2 mg (50.6%). **$C_{22}H_{40}P_2Rh_2$ (572.32 g mol^{-1}):** calc. C 46.17 %, H 7.04 %; found C 46.78 %, H 6.70%. **^{1}H NMR (500 MHz, 298K, C_6D_6) δ:** 4.66 (s, 4H, C*H* (cod)), 4.01 (s, 4H, C*H* (cod)), 2.18 (m, 8H, C*H$_2$* (cod)), 2.00 (m, 8H, C*H$_2$* (cod)), 1.27 (dd, 12H, $^{2}J_{P-H}$ 7.3 Hz, $^{3}J_{Rh-H}$ 1.0 Hz P*Me*), 0.92 (m, 4H, PC*H$_2$*). **^{13}C{^{1}H} NMR (125.8 MHz, 298K, C_6D_6) δ:** 92.17 (m, *C*H (cod)), 78.54 (d, $^{2}J_{P-C}$ 9 Hz, *C*H (cod)), 32.56 (s, *C*H$_2$ (cod)), 31.28 (s, *C*H$_2$ (cod)), 19.90 (d, $^{1}J_{P-C}$ 19 Hz, P*Me*), 18.06 (d, $^{1}J_{P-C}$ 28 Hz, P*C*H$_2$). **^{31}P{^{1}H} NMR (202.5 MHz, 298K, C_6D_6) δ:** –6.69 (dt, $^{1}J_{Rh-P}$ 154.3 Hz, *P*Me$_2$).

[{κ^2*P,P*-$Cl_2Al(CH_2PMe_2)_2$}Ir(cod)] (5): A solution of $(Me_2PCH_2AlMe_2)_2$ (15.0 mg, 0.0567 mmol) in 1 mL of toluene was added to [{IrCl(cod)}$_2$] (77.7 mg, 0.113 mmol) in 2 mL of toluene. The deep red solution was stirred at 25°C for 3 hours. The deep red solution was decanted from a dark burgundy oil, and the solvent was removed in vacuo, leaving behind a solid. The product was then recrystallized from a concentrated solution of 1,2-difluorobenzene layered with hexanes (1:1) at –30°C to obtain clear, burgundy X-ray quality crystals of **5**. The recrystallized yield was 12.5 mg (40.1 %)). $C_{14}H_{28}AlCl_2P_2Ir$ (548.43 g mol^{-1}): calcd. C 30.66 %, H 5.15 %; found C 30.92 %, H 4.83 %. **^{1}H NMR (500 MHz, 298K, C_6D_6) δ:** 3.76 (m, 4H, C*H* (cod)), 1.70 (m, 4H, C*H$_2$* (cod)), 1.49 (m, 4H, C*H$_2$* (cod)), 0.95 (d, 12H, $^{2}J_{P-H}$ 9.0 Hz, P*Me$_2$*), 0.75 (d, 12H, $^{2}J_{P-H}$ 13.0 Hz, PC*H$_2$*Al). **^{13}C{^{1}H} NMR (125.8 MHz, 298K, C_6D_6) δ:** 79.81 (t, $^{2}J_{P-C}$ = 6.3 Hz, *C*H (cod)), 31.59 (s, *C*H$_2$ (cod)), 16.81 (m, P*Me*), 13.95 (located from 2D NMR spectra, P*C*H$_2$Al). **^{31}P{^{1}H} NMR (202.5 MHz, 298K, C_6D_6) δ:** –13.08 (s).

[{κ^2*P,P*-$Cl_2Al(CH_2PMe_2)_2$}Rh(cod)] (6): A solution of {$(Me_2PCH_2)_2AlCl$}$_2$ (19.3 mg, 0.091 mmol) in 1 mL of benzene was added to [{RhCl(cod)}$_2$] (22.2 mg, 0.045 mmol) in 2 mL of benzene, and the resulting mixture was stirred at room temperature for 1 h. NMR spectroscopy indicated the product was formed in a qualitative yield. The resulting vibrant orange solution was left at room temperature for 12 hours, at which point orange crystals of **6** formed. The mother liquor was decanted and the crystals were dried in vacuo. The recrystallized yield was 23.1 mg (55 %). **$C_{14}H_{28}AlCl_2P_2Rh$ (459.12 g mol^{-1}):** calcd. C 36.63 %, H 6.15 %; found C 36.88 %, H 6.18 %. **^{1}H NMR (500 MHz, 298K, CD_2Cl_2) δ:** 4.78 (s, 4H, CH (cod)), 2.32 (m, 8H, CH2 (cod)), 1.38 (d, 12H, $^{2}J_{P-H}$ 7.5 Hz, PMe), 0.55 (d, 4H, $^{2}J_{P-H}$ 10.2 Hz, PCH$_2$Al). **^{13}C{1H} NMR (125.8 MHz, 298K, CD_2Cl_2) δ:** 93.97 (m, CH (cod)), 31.19 (s, CH$_2$ (cod)), 18.01 (dd, $^{1}J_{P-C}$ = 11.3, 13.8 Hz, PMe$_2$), 13.60 (bs, PCH$_2$Al). **^{31}P{1H} NMR (202.5 MHz, 298K, CD_2Cl_2) δ:** –6.60 (d, $^{1}J_{Rh-P}$ 139.7 Hz, *P*Me$_2$).

[(PtMe{μ-κ^1*P*:κ^2*P,P*-$MeAl(CH_2PMe_2)_3$})$_2$] (7): A solution of $(Me_2PCH_2AlMe_2)_2$ (111.2 mg, 0.4207 mmol) in 2 mL of toluene was added to [$PtMe_2$(cod)] (93.5 mg, 0.2805 mmol) in 2 mL of toluene. The clear and colorless solution was stirred at 75°C for 12 hours. The solvent was evacuated from the pale beige solution, leaving behind a pale beige solid. Slow evaporation of a benzene solution at 25°C afforded clear, colourless X-ray quality crystals of **7** (112.5 mg; 42 % yield). **$C_{22}H_{60}Al_2P_6Pt_2$ (954.69 g mol^{-1}):** calcd. C 27.68, H 6.33%; found C 27.52, H 6.09%. **^{1}H NMR (600 MHz, 298K, CD_2Cl_2) δ:** 1.60 (q, 6H, 2JP-H 8 Hz, PMe2), 1.42 (m, 24H, PMe$_2$), 1.20 (q, 6H, $^{2}J_{P-H}$ 10 Hz, PMe$_2$), 0.95 (m, 2H, PCH$_2$Al), 0.53 (m, 4H, PCH$_2$Al), 0.07-0.27 (m, 6H, PCH$_2$Al), 0.18 (m, 6H, PtMe), –1.05 (s, 6H, AlMe). **^{13}C{^{1}H} NMR (150.9 MHz, 298K, CD_2Cl_2) δ**: 25.11 (d, $^{1}J_{P-C}$ 21 Hz, PMe$_2$), 22.48 (d, $^{1}J_{P-C}$ 21 Hz, PMe$_2$), 21.26 (d, $^{1}J_{P-C}$ 36 Hz, PMe$_2$), 20.45 (d, $^{1}J_{P-C}$ 27 Hz, PMe$_2$), 17.74 (d, $^{1}J_{P-C}$ 40 Hz, PMe$_2$), 14.83 (d, $^{1}J_{P-C}$ 34 Hz, PMe$_2$), –2.69 (d, $^{1}J_{P-C}$ 77 Hz, PtMe) (PCH$_2$Al signals and ^{195}Pt satellites were not observed in the ^{13}C{1H} NMR spectrum due to the low solubility of compound **7**). **^{31}P{^{1}H} NMR (242.9 MHz, 298K, CD_2Cl_2) δ:** –10.14 (t, $^{2}J_{P-P}$,cis 23 Hz, $^{1}J_{Pt-P}$ = 1827 Hz), –11.53 (dd, $^{2}J_{P-P}$,cis 23 Hz, $^{2}J_{P-P}$,trans 398 Hz, $^{1}J_{Pt-P}$ 2354 Hz), –13.59 (dd, $^{2}J_{P-P}$,cis 23 Hz, $^{2}J_{P-P}$,trans 398 Hz, $^{1}J_{Pt-P}$ 2406 Hz) (^{31}P chemical shifts and $^{2}J_{P-P}$ couplings obtained from simulated data; $^{1}J_{Pt,P}$ couplings determined directly from the NMR spectrum). **^{195}Pt NMR (107.5 MHz, 298K, C_6D_6) δ:** –4741.6 (ddd, $^{1}J_{Pt-P(a)}$ = 2421 Hz, $^{1}J_{Pt-P(b)}$ = 2376 Hz, $^{1}J_{Pt-P(c)}$ = 1830 Hz; $^{1}J_{Pt,P}$ couplings determined directly from the NMR spectrum; P(a) and P(b) are trans to one another; P(c) is trans to the methyl group).

Reaction of $(Me_2PCH_2AlMe_2)_2$ with [AuCl(CO)]: A solution of $(Me_2PCH_2AlMe_2)_2$ (9.3 mg, 0.0352 mmol) in 0.3 mL C_6D_6 was added to AuCl(CO) (18.6 mg, 0.0704 mmol) in 0.3 mL C_6D_6. The solution immediately precipitated a dark blue-black solid, with some gold mirror forming on the walls of the vial. The

precipitate was allowed to settle, and the clear, colorless supernatant was decanted. The black powder was washed three times with hexanes and dried in vacuo. The black solid was shown to consist of elemental gold by PXRD. Slow evaporation of the clear, colorless supernatant yielded colorless crystals, which were characterized as $(Me_2PCH_2AlMeCl)_2$ by XRD. **^{1}H NMR (600 MHz, 298K, C_6D_6) δ:** 1.03 (d, 3H $^2J_{P\text{-}H}$ = 9.2 Hz, P*Me***), 0.93 (d, 6H $^2J_{P\text{-}H}$ = 8.6 Hz, P*Me**), 0.79 (d, 6H $^2J_{P\text{-}H}$ = 8.8, P*Me**), 0.61 (d, 3H $^2J_{P\text{-}H}$ = 8.4 Hz, P*Me***), 0.20 (m, 1H, CH_2**), 0.04 (m, 4H, CH_2*), –0.18 (m, 1H, CH_2**), –0.36 (d, 6H, $^3J_{P\text{-}H}$ = 4.3 Hz, Al*Me**), –0.42 (d, 3H, $^3J_{P\text{-}H}$ = 4.3 Hz, Al*Me***). Integrations are taken directly from the ^{1}H NMR spectrum, so are reflective of the 2:1 ratio ratio of the diastereomers. **^{13}C{^{1}H} NMR (125.8 MHz, 298K, C_6D_6) δ:** 13.25 (d, $^1J_{P\text{-}C}$ = 22.9 Hz, P*Me**), 11.93 (d, $^1J_{P\text{-}C}$ = 23.4, P*Me***), 11.77 (d, $^1J_{P\text{-}C}$ = 24.9 Hz, P*Me***), 10.49 (d, $^1J_{P\text{-}C}$ = 27.1 Hz, P*Me**), 5.1 (CH_2 for both diastereomers; identified from the 2D NMR spectra), –8.5 (Al*Me***, identified from the 2D NMR spectra), –8.9 (Al*Me**, identified from the 2D NMR spectra). **^{31}P{^{1}H} NMR (202.5 MHz, 298K, C_6D_6) δ:** –41.4 (broad). * major diastereomer, ** minor diastereomer

Reaction of $(Me_2PCH_2AlMe_2)_2$ with $[PtCl_2(cod)]$: A solution of $(Me_2PCH_2AlMe_2)_2$ (9.1 mg, 0.0344 mmol) in 0.3 mL C_6D_6 was added to $PtCl_2$(cod) (12.9 mg, 0.0344 mmol) in 0.3 mL C_6D_6. The mixture was monitored by NMR spectroscopy at room temperature over the course of two days.

References

1 K. M. Paskaruk, B. E. Cowie and D. J. H. Emslie, in Comprehensive Coordination Chemistry III, ed. E. C. Constable, G. Parkin, L. Que, Jr., Elsevier, 2021, vol. 1, pp. 717.

2 G. Bouhadir and D. Bourissou, *Chem. Soc. Rev.*, 2016, **45**, 1065.

3 A. Amgoune, G. Bouhadir and D. Bourissou, *Top. Curr. Chem.*, 2013, **334**, 281.

4 H. Kameo and H. Nakazawa, *Chemistry-an Asian Journal*, 2013, **8**, 1720.

5 J. Bauer, H. Braunschweig and R. D. Dewhurst, *Chem. Rev.*, 2012, **112**, 4329.

6 D. L. Grimmett, J. A. Labinger, J. N. Bonfiglio, S. T. Masuo, E. Shearin and J. S. Miller, *J. Am. Chem. Soc.*, 1982, **104**, 6858.

7 J. A. Labinger and J. S. Miller, *J. Am. Chem. Soc.*, 1982, **104**, 6856.

8 J. A. Labinger, J. N. Bonfiglio, D. L. Grimmett, S. T. Masuo, E. Shearin and J. S. Miller, *Organometallics*, 1983, **2**, 733.

9 D. L. Grimmett, J. A. Labinger, J. N. Bonfiglio, S. T. Masuo, E. Shearin and J. S. Miller, *Organometallics*, 1983, **2**, 1325.

10 F.-G. Fontaine and D. Zargarian, *J. Am. Chem. Soc.*, 2004, **126**, 8786.

11 M. H. Thibault, J. Boudreau, S. Mathiotte, F. Drouin, O. Sigouin, A. Michaud and F.-G. Fontaine, *Organometallics*, 2007, **26**, 3807.

12 J. Boudreau and F.-G. Fontaine, *Organometallics*, 2011, **30**, 511.

13 M. Devillard, E. Nicolas, C. Appelt, J. Backs, S. Mallet-Ladeira, G. Bouhadir, J. C. Slootweg, W. Uhl and D. Bourissou, *Chem. Commun.*, 2014, **50**, 14805.

14 M. Devillard, E. Nicolas, A. W. Ehlers, J. Backs, S. Mallet-Ladeira, G. Bouhadir, J. C. Slootweg, W. Uhl and D. Bourissou, *Chem. Eur. J.*, 2015, **21**, 74.

15 M. Devillard, R. Declercq, E. Nicolas, A. W. Ehlers, J. Backs, N. Saffon-Merceron, G. Bouhadir, J. C. Slootweg, W. Uhl and D. Bourissou, *J. Am. Chem. Soc.*, 2016, **138**, 4917.

16 M. Sircoglou, G. Bouhadir, N. Saffon, K. Miqueu and D. Bourissou, *Organometallics*, 2008, **27**, 1675.

17 M. Sircoglou, N. Saffon, K. Miqueu, G. Bouhadir and D. Bourissou, *Organometallics*, 2013, **32**, 6780.

18 J. Fajardo and J. C. Peters, *Inorg. Chem.*, 2021, **60**, 1221.

19 Q. H. Lai, M. N. Cosio and O. V. Ozerov, *Chem. Commun.*, 2020, **56**, 14845.

20 Q. H. Lai, N. Bhuvanesh, J. Zhou and O. V. Ozerov, *Dalton Trans.*, 2021, **50**, 5776.

21 B. E. Cowie, F. A. Tsao and D. J. H. Emslie, *Angew. Chem. Int. Ed.*, 2015, **54**, 2165.

22 T. Saito, N. Hara and Y. Nakao, *Chem. Lett.*, 2017, **46**, 1247.

23 N. Hara, T. Saito, K. Semba, N. Kuriakose, H. Zheng, S. Sakaki and Y. Nakao, *J. Am. Chem. Soc.*, 2018, **140**, 7070.

24 K. Semba, I. Fujii and Y. Nakao, *Inorganics*, 2019, **7**.

25 I. Fujii, K. Semba, Q. Z. Li, S. Sakaki and Y. Nakao, *J. Am. Chem. Soc.*, 2020, **142**, 11647.

26 N. Hara, N. Uemura and Y. Nakao, *Chem. Commun.*, 2021, **57**, 5957.

27 R. Seki, N. Hara, T. Saito and Y. Nakao, *J. Am. Chem. Soc.*, 2021, **143**, 6388.

28 K. Semba, F. Shimoura and Y. Nakao, *Chem. Lett.*, 2022, **51**, 455.

29 P. A. Rudd, S. S. Liu, L. Gagliardi, V. G. Young and C. C. Lu, *J. Am. Chem. Soc.*, 2011, **133**, 20724.

30 P. A. Rudd, N. Planas, E. Bill, L. Gagliardi and C. C. Lu, *Eur. J. Inorg. Chem.*, 2013, 3898.

31 R. C. Cammarota and C. C. Lu, *J. Am. Chem. Soc.*, 2015, **137**, 12486.

32 A. B. Thompson, D. R. Pahis, V. Bernales, L. C. Gallington, C. D. Malonzo, T. Webber, S. J. Tereniak, T. C. Wang, S. P. Desai, Z. Y. Li, I. S. Kim, L. Gagliardi, R. L. Penn, K. W. Chapman, A. Stein, O. K. Farha, J. T. Hupp, A. B. F. Martinson and C. C. Lu, *Chem. Mater.*, 2016, **28**, 6753.

33 J. T. Moore, N. E. Smith and C. C. Lu, *Dalton Trans.*, 2017, **46**, 5689.

34 M. V. Vollmer, J. Xie and C. C. Lu, *J. Am. Chem. Soc.*, 2017, **139**, 6570.

35 M. V. Vollmer, J. Xie, R. C. Cammarota, V. G. Young, E. Bill, L. Gagliardi and C. C. Lu, *Angew. Chem. Int. Ed.*, 2018, **57**, 7815.

36 R. C. Cammarota, J. Xie, S. A. Burgess, M. V. Vollmer, K. D. Vogiatzis, J. Y. Ye, J. C. Linehan, A. M. Appel, C. Hoffmann, X. P. Wang, V. G. Young and C. C. Lu, *Chem. Sci.*, 2019, **10**, 7029.

37 M. V. Vollmer, R. C. Cammarota and C. C. Lu, *Eur. J. Inorg. Chem.*, 2019, 2140.

38 M. V. Vollmer, J. Y. Ye, J. C. Linehan, B. J. Graziano, A. Preston, E. S. Wiedner and C. C. Lu, *Acs Catalysis*, 2020, **10**, 2459.

39 B. J. Graziano, M. V. Vollmer and C. C. Lu, *Angew. Chem. Int. Ed.*, 2021, **60**, 15087.

40 M. D. Fryzuk, N. T. McManus, S. J. Rettig and G. S. White, *Angew. Chem. Int. Ed. Engl.*, 1990, **29**, 73.

41 M. D. Fryzuk, L. Huang, N. T. McManus, P. Paglia, S. J. Rettig and G. S. White, *Organometallics*, 1992, **11**, 2979.

42 O. T. Beachley, M. A. Banks, J. P. Kopasz and R. D. Rogers, *Organometallics*, 1996, **15**, 5170.

43 F. Bessac and G. Frenking, *Inorg. Chem.*, 2006, **45**, 6956.

44 S. Dutta, S. M. De, S. Bose, E. Mahal and D. Koley, *Eur. J. Inorg. Chem.*, 2020, 638.

45 D. M. C. Ould, J. L. Carden, R. Page and R. L. Melen, *Inorg. Chem.*, 2020, **59**, 14891.

46 Several chromium complexes containing an $R_2PNR'AlR''_2$ unit have been generated in situ, including $[Cr(\mu\text{-}Cl)_2(PPh_2N^tBuAlR_2)_2]$ (R = Me or Et): (a) I. Thapa, S. Gambarotta, I. Korobkov, R. Duchateau, S. V. Kulangara and R. Chevalier, *Organometallics*, 2010, **29**, 4080.; (b) A. Alzamly, S. Gambarotta and I. Korobkov, *Organometallics*, 2014, **33**, 1602.

47 H. H. Karsch, A. Appelt, F. H. Kohler and G. Muller, *Organometallics*, 1985, **4**, 231.

48 B. Cordero, V. Gómez, A. E. Platero-Prats, M. Revés, J. Echeverría, E. Cremades, F. Barragán and S. Alvarez, *Dalton Trans.*, 2008, 2832.

49 J. C. Thomas and J. C. Peters, *Inorg. Chem.*, 2003, **42**, 5055.

50 A. Tamaki and J. K. Kochi, *J. Organometal. Chem.*, 1973, **61**, 441.

51 S. Komiya, T. A. Albright, R. Hoffmann and J. K. Kochi, *J. Am. Chem. Soc.*, 1977, **99**, 8440.

52 J. Miranda-Pizarro, Z. W. Luo, J. J. Moreno, D. A. Dickie, J. Campos and T. B. Gunnoe, *J. Am. Chem. Soc.*, 2021, **143**, 2509.

53 $[Me_2PCH_2AlMe_2]_2$ has been shown to be an effective initiator for polymerization of Michael-type monomers, likely involving reactivity at the Al-CH_2 linkage: M. Weger, R. K. Grotsch, M. G. Knaus, M. M. Giuman, D. C. Mayer, P. J. Altmann, E. Mossou, B. Dittrich, A. Pothig and B. Rieger, *Angew. Chem. Int. Ed.*, 2019, **58**, 9797.

54 H. H. Karsch, A. Appelt and G. Muller, *Organometallics*, 1985, **4**, 1624.

55 E. Costa, P. G. Pringle and M. Ravetz, *Inorg. Synth.*, 1997, **31**, 284.

56 G. M. Sheldrick, *Acta Crystallogr., Sect. A: Found. Crystallogr.*, 2008, **64**, 112.

57 G. M. Sheldrick, *Acta Crystallogr., Sect. A: Found. Crystallogr.*, 2015, **71**, 3.

58 G. M. Sheldrick, *Acta Crystallogr., Sect. C: Struct. Chem.*, 2015, **71**, 3.

59 O. V. Dolomanov, L. J. Bourhis, R. J. Gildea, J. A. K. Howard and H. Puschmann, *J. Appl. Crystallogr.*, 2009, **42**, 339.